Author Manuscript

Title: Facile Access to Organostibines via Selective Organic Superbase Catalyzed Antimony-Carbon Protonolysis

Authors: Clemens Krempner; Jacob Culvyhouse; Daniel Unruh; Hans Lischka; Adelia Aquino

To be cited as: 10.1002/anie.202407822

Link to VoR: https://doi.org/10.1002/anie.202407822

WILEY VCH

RESEARCH ARTICLE

Highly Selective Antimony-Carbon Bond Formation through Organic Superbase Catalysis – Facile Access to Organostibines under Metal- and Salt-Free Conditions

Jacob Culvyhouse,[a] Daniel K. Unruh,[a] Hans Lischka,[a] Adelia J.A. Aquino,[b] Clemens Krempner*[a]

[a] J. Culvyhouse, Dr. D.K. Unruh, Prof. Dr. H. Lischka, Prof. Dr. C. Krempner
Department of Chemistry & Biochemistry
Texas Tech University
Memorial Dr. & Boston, Lubbock, Texas, 79409, United States
E-mail: Clemens.krempner@ttu.edu

[b] Prof. Dr. A.J.A. Aquino
Department of Mechanical Engineering
Texas Tech University
Lubbock, Texas, 79409-1021, United States.

Abstract: The selective formation of antimony-carbon bonds via organic superbase catalysis under metal- and salt-free conditions is reported. This novel approach utilizes electron-deficient stibine, $Sb(C_6F_5)_3$, to give upon base-catalyzed reactions with weakly acidic aromatic and heteroaromatic hydrocarbons facile access to a range of new aromatic and heteroaromatic stibines, respectively, with loss of C_6F_5H. Moreover, also the significantly less electron-deficient stibines, $Ph_2SbC_6F_5$ and $PhSb(C_6F_5)_2$ smoothly underwent base-catalyzed exchange reactions with a range of terminal alkynes to generate the stibines of formulae $PhSb(C{\equiv}CPh)_2$, and $Ph_2SbC{\equiv}CR$ [R = C_6H_5, C_6H_4-NO_2, COOEt, CH_2Cl, CH_2NEt_2, CH_2OSiMe_3, $Sb(C_6H_5)_2$], respectively. These formal substitution reactions proceed with high selectivity as only the C_6F_5 groups serve as a leaving group to be liberated as C_6F_5H upon formal proton transfer from the alkyne. Kinetic studies of the base-catalyzed reaction of $Ph_2SbC_6F_5$ with phenyl acetylene to form $Ph_2SbC{\equiv}CPh$ and C_6F_5H suggested the empirical rate law to exhibit a first-order dependence with respect to the base catalyst, alkyne and stibine. DFT calculations support a pathway proceeding via a concerted σ-bond metathesis transition state, where the base catalyst activates the Sb-C_6F_5 bond sequence through secondary bond interactions.

Introduction

The last decade has witnessed an increased interest in the chemistry of tri- and pentavalent organoantimony compounds with potential applications ranging from anion binding [1], sensing [2], and transport [3] to optical materials [4] and as Z-type ligands in support of late transition metals for catalysis [5]. Moreover, highly electrophilic neutral and cationic antimony (III) and (V) species were reported to be capable of activating small molecules [6] and catalyzing a range of organic reactions via Lewis acid-type catalysis [7, 8]. For example, Matile's group demonstrated that electron-deficient organostibines such as $Sb(C_6F_5)_3$ can activate polar organic substrates through weak secondary bond interactions between the substrate and the antimony center. These findings enabled antimony-catalyzed Reissert-type substitution as well as brevetoxin-type polyether cyclization to proceed with high selectivities [8a-d]. Later, Jemmis and Venugopal applied more electrophilic cationic aryl stibines to catalyze cross-carbonyl and ring-closing olefin metathesis [8e]. In addition to being used as catalysts, organostibines have found applications as nucleophilic reagents for cross-coupling reactions via palladium catalysis [9]. Qiu and co-workers showed that specifically designed benchtop stable 5-aza-stibocines can be utilized as reagents for catalytic C-C, C-S, and C-Se bond formation to give a wide range of unsymmetrical diaryl methanes, functionalized biphenyls as well as chalcogenated olefins and ethers [10]. Despite these synthetic advances, broader applications of organoantimony chemistry in fields such as catalysis and material chemistry will require expanding the synthetic toolbox to milder and more selective methods of generating antimony-carbon bonds. In particular, catalytic methods have the potential to open new avenues to the selective synthesis of organostibines with increased structural complexity, which are difficult to synthesize with currently available methods involving highly reactive air- and moisture-sensitive organometallic reagents [11]. However, very few examples exist of methods involving catalytic Sb-C bond formation, while metal-free catalytic methods are virtually unknown (Scheme 1).

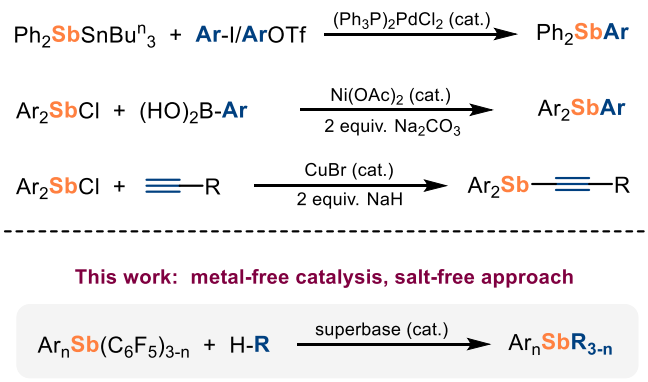

Scheme 1. Catalytic Sb-C bond formation approaches.

In an early report, the synthesis of various triaryl-substituted stibines was reported through palladium-catalyzed Stille cross-coupling of in situ prepared and air-sensitive stannyl stibines, $Bu_3SnSbPh_2$, with aryl iodides or triflates [12]. More recently, the Ni-catalyzed cross-coupling of chloro-stibines with aryl/alkyl boronic acids or alkyl chlorides was disclosed [13]. In a related study, chloro-stibines could be coupled with terminal alkynes to form Sb-C bonds via copper catalysis [14], requiring, however, two equivalents of NaH as a base.

Concerning the design of novel frustrated Lewis pairs (FLPs) [15] as catalysts for metal-free hydrogenations, our group came recently across $Sb(C_6F_5)_3$ as a potentially useful weak Lewis acid component [16]. While $Sb(C_6F_5)_3$ does not react with bulky organic superbases, we discovered that it smoothly undergoes an organic superbase-catalyzed exchange reaction in the presence of carbon-based nucleophiles resulting in the formation of new organostibines via C-H bond activation [17, 18]. This unprecedented base-catalyzed, metal- and salt-free process enables the selective synthesis of a wide range new aromatic-, heteraromatic- and alkynyl-substituted organostibines.

Results and Discussion

As mentioned above, we initially investigated the ability of $Sb(C_6F_5)_3$ (**1**) to act as a weak Lewis acid component in frustrated Lewis pair chemistry (FLP) [19]. However, with limited success, $Sb(C_6F_5)_3$ when combined with various bulky organic superbases (Scheme 2) did not engage in heterolytic hydrogen cleavage. In contrast, interactions with an excess of phenyl acetylene (pK_a = 28.8 in DMSO) [20] led to an instant reaction with quantitative formation of pentafluorobenzene, C_6F_5H, as confirmed by solution ^1H and ^{19}F NMR spectroscopy. Simultaneously, a crystalline material precipitated, which by NMR spectroscopy and X-ray crystallography was identified as the previously reported tris(phenylethynyl)stibine **2** (Scheme 1) [21]. Inspection of the reaction mixture by ^{31}P NMR spectroscopy revealed no change in the chemical shifts of the respective phosphorous signals related to the phosphazene bases suggesting that the quantitative formation of stibine **2** to have occurred through base-catalysis [22]. Indeed, when one equiv. of $Sb(C_6F_5)_3$ (**1**) was treated with three equiv. of phenyl acetylene in the presence of catalytic amounts of either **P₂-Et**, **P₂-Bu^t**, or **P₄-Bu^t**, stibine **2** was smoothly formed as the sole product at room temperature in less than 15 minutes (Table 1). The Verkade bases **V-Me**, **V-Bu^i**, and **V-Pr^i** showed somewhat lower activity but still converted $Sb(C_6F_5)_3$ to **2** quantitatively in less than 24 hours (Table S1). Even with the weaker phosphazene base **P₁-Bu^t**, the reaction was complete in less than 24 hours, while guanidine **G**, most likely due to its lower basicity showed only 64% conversion after 24 hours.

Encouraged by these findings, we wondered whether this unprecedented base-catalyzed Sb-C bond formation process could be extended to the selective synthesis of so far unknown stibines with heterocyclic substituents. We initially chose oxazole (pK_a = 27.1 in DMSO) and thiazole (pka = 29.5 in DMSO), because these heteroaromatic hydrocarbons have C-H bond acidities [23] similar to that of phenyl acetylene. In both cases, reactions with $Sb(C_6F_5)_3$ and 5 mol% of **P₂-Bu^t** went smoothly, to generate upon gentle heating precipitates with nearly quantitative formation of three equivalents of C_6F_5H as confirmed by ^1H and ^{19}F NMR spectroscopy. However, both precipitates assumed to be $Sb(thiazolyl)_3$ and $Sb(oxazolyl)_3$ were insoluble in nonpolar and polar organic solvents including DMF, pyridine, and DMSO, rendering their structural characterization impossible.

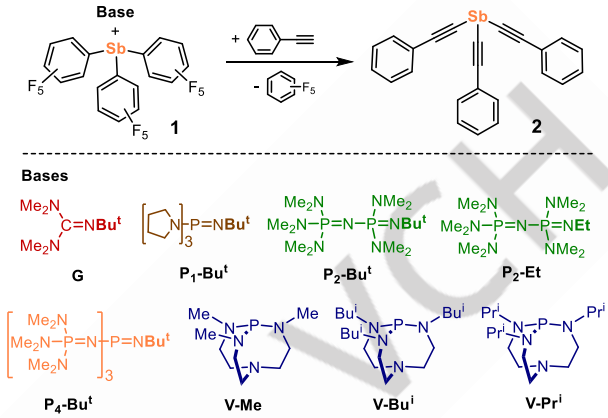

Scheme 2. Base-catalyzed transformation of $Sb(C_6F_5)_3$ (**1**) to $Sb(C{\equiv}C\text{-}Ph)_3$ (**2**).

Table 1. Screening of bases for the catalytic conversion of $Sb(C_6F_5)_3$ (**1**) to $Sb(C{\equiv}C\text{-}Ph)_3$ (**2**)[a].

base	pK_a[b]	Cat. load. [mol%]	T [°C]	t [min]	Conv.[c] [%]
G	24	5	25	15	7
P₁-Bu^t	28	5	25	15	65
V-Me	33	5	25	15	69
V-Bu^i	34	5	25	15	73
V-Pr^i	34	5	25	15	73
P₂-Et	34	5	25	15	99
P₂-Bu^t	33	5	25	15	99
P₄-Bu^t	42	5	25	15	99

[a] Conditions: 0.642 mmol $Sb(C_6F_5)_3$, 1.941 mmol phenyl acetylene, 5 mol % base. 4 ml toluene; [b] values relate to the pK_a values of the corresponding acid; [c] conversions were determined by ^{19}F NMR spectroscopy.

To circumvent issues associated with the formation of insoluble products, benzothiazole (pK_a = 27.3 in DMSO), and benzoxazole (pK_a = 24.8 in DMSO) [23], were treated with $Sb(C_6F_5)_3$ and **P₂-Bu^t** as the catalyst, resp., in toluene as the solvent. In both cases, the corresponding trisubstituted stibines **3** and **4** could be synthesized and isolated as crystalline materials. The analogous reaction of $Sb(C_6F_5)_3$ with less acidic 1-methyl-benzimidazole (pK_a = 32.5 in DMSO) [21] and **P₂-Bu^t** (5 mol%) required more forcing

conditions and a six-fold excess of the imidazole to accomplish the formation of the respective stibine **5**. Furthermore, the reactions of $Sb(C_6F_5)_3$ with 5-phenyl-thiazole and 5-phenyl-oxazole, respectively, in the presence of 5 mol% of **P₂-Bu^t** proceeded smoothly as well to give the heterocyclic stibines **6** (70% yield) and **7** (60% yield) as thermally stable, colorless solids. However, regardless of the bases used, the heterocycles furan (pK_a = 35.0 in DMSO) and thiophene (pK_a = 32.5 in DMSO) [23] did not engage in the base-catalyzed Sb-C bond formation, most likely due to their lower acidity compared to the thiazol and oxazole derivatives (vide supra). Gratifyingly, the treatment of 2-cyano-thiophene with $Sb(C_6F_5)_3$ and **P₂-Bu^t** (5 mol%) gave rise to the formation of **8** in 85% isolated yields. Introducing a cyano group in the 2-position of thiophene appears to enhance the acidity to an extent at which base-induced C-H bond activation is feasible, enabling the selective formation of the Sb-C bonds Stibines **3-8** were fully characterized by elemental analysis, NMR-, and IR-spectroscopy and combustion analysis. In addition, the solid-state structures of **3**, **4** and **8** were determined by single-crystal X-ray crystallography (Figure 1).

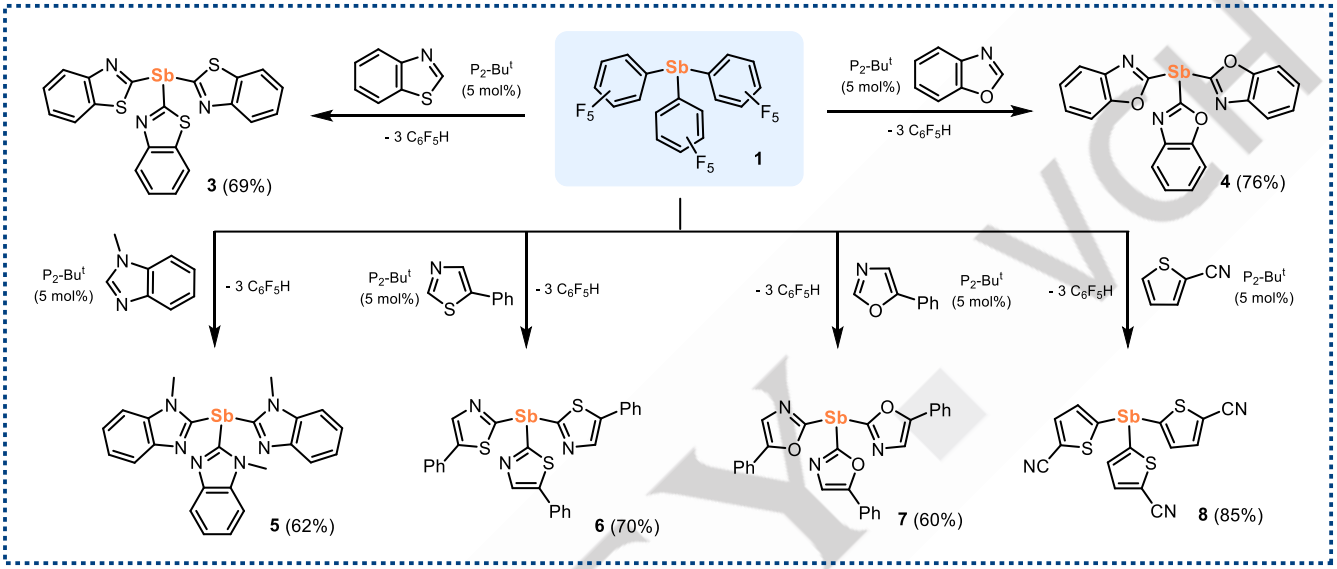

Scheme 3. Base-catalyzed formation of **3-8**.

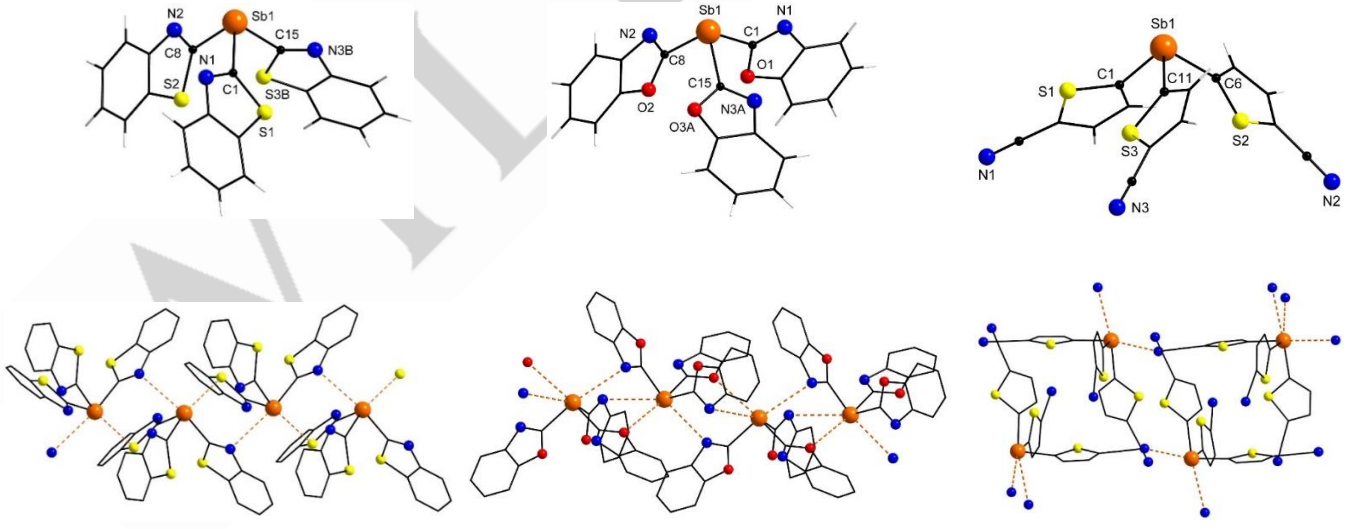

Figure 1. The solid-state structures of **3**, **4** and **8**. Selected bond lengths [Å] and angles [°]: **3**, Sb1 C1 2.166(2), Sb1 C8 2.165(2), Sb1 C15 2.182(2), S1 C1 1.752(2), S2 C8 1.763(2), S3A C15 1.767(2), N3A C15 1.277(4), N1 C1 1.306(3), N2 C8 1.294(3), C1 Sb1 C15 89.2(1), C8 Sb1 C1 89.1(1), C8 Sb1 C15 88.1(1); **4**, Sb1 C1 2.164(3), Sb1 C8 2.159(2), Sb1 C15 2.153(3), O1 C1 1.377(3), O2 C8 1.371(3), O3A C15 1.364(7), N3A C15 1.300(9), N1 C1 1.291(3), N2 C8 1.299(3), C8 Sb1 C1 91.6(1), C15 Sb1 C1 87.3(1), C15 Sb1 C8 93.7(1); **8**, Sb1 C1 2.161(5), Sb1 C6 2.170(5), Sb1 C11 2.148(5), C1 Sb1 C6 91.0(2), C11 Sb1 C1 93.5(2), C11 Sb1 C6 93.0(2).

The results of the single-crystal X-ray analysis of **3** (Figure 1) further confirmed its connectivity with Sb-C bonds and C-Sb-C angles within the narrow range of 2.17-2.18 Å and 88°-89°, respectively. In the solid state, **3** features an infinite chain structure where the monomeric subunits are held together through secondary bond interaction (pnictogen bonding) between the antimony and the heterocyclic donor atoms [24]. Each of the antimony centers in the chain binds to nitrogen and sulfur from the two neighboring monomeric subunits resulting in a distorted square-pyramidal coordination environment for antimony with N···Sb···S angles of about 99°. The respective Sb···N and Sb···S distances were found to be 3.18 Å and 3.21 Å, markedly below the sum of the SbS (ca. 3.86 Å) and SbN (ca. 3.61 Å) Van der Waals radii [25]. A similar structural arrangement was noticed for **4** (Figure 1), again with an infinite chain structure through pnictogen bonding between the oxygen and nitrogen donors of the neighboring subunits, and Sb-C bonds and C-Sb-C angles ranging from 2.15-2.16 Å and 87°-94°, resp. However, in this case, two nitrogen and one oxygen serve as pnictogen donors giving rise to a distorted octahedral coordination environment for every antimony center (3-point binding). The respective pnictogen bonds were found to be 3.33 and 3.26 Å [Sb···N] and 3.31 Å [Sb···O], again all were well below the sum of the SbO (ca. 3.58 Å) and SbN (ca. 3.61 Å) Van der Waals radii [25]. The respective bond parameters of **8** are very similar to **3** and **4** with central Sb-C bonds and C-Sb-C angles ranging from 2.15-2.17 Å and 91°-94°, respectively (Figure 1). Again, pnictogen bonding occurs between the antimony centers and the cyano nitrogen atoms leading to extended network structures in the solid state. The Sb···N contacts range from 2.91-3.29 Å creating a distorted square-pyramidal coordination environment for each antimony center.

To further extend the scope of this novel catalytic approach toward the selective formation of Sb-C bonds, efforts were undertaken to synthesize unknown tris(fluorenyl)stibine, $Sb(C_{13}H_9)_3$. However, when three equivalents of fluorene (pK_a = 22.0 in DMSO) [20] were treated with $Sb(C_6F_5)_3$ under base catalysis, the desired product $Sb(C_{13}H_9)_3$ was not observed even at elevated temperatures, rather bis(fluorenyl)stibine **9** was formed as the sole product (Scheme 4).

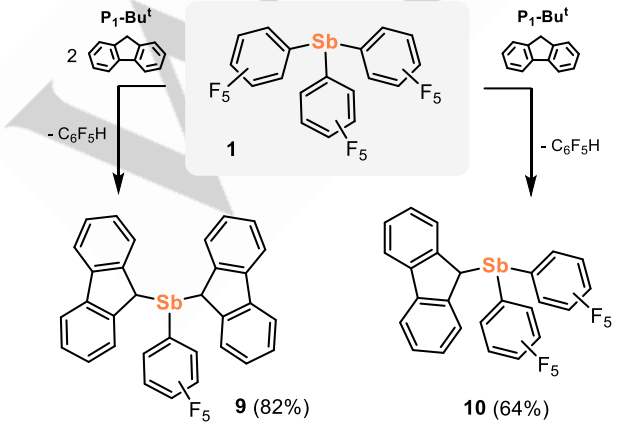

Scheme 4. Base-catalyzed formation of **9** and **10**.

Best yields of **9** were obtained when only two equivalents of fluorene were employed. Treating $Sb(C_6F_5)_3$ with only one equivalent of fluorene yielded the mono-substituted stibine **10** again with high selectivity and good isolated yields. Both stibines are thermally stable crystalline materials that were fully characterized by ^1H and ^{13}C NMR spectroscopy, combustion analysis, and single-crystal X-ray crystallography (Figure 2).

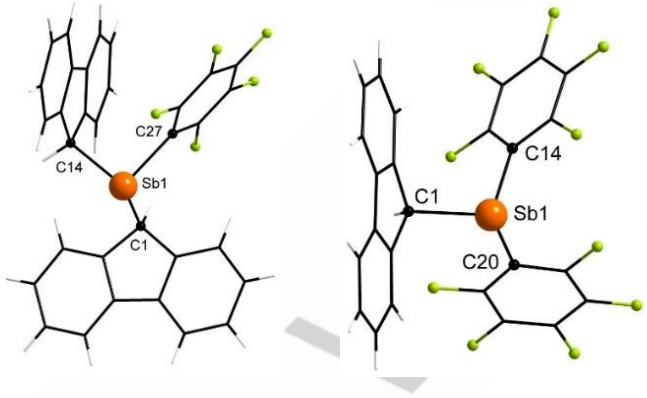

Figure 2. Solid-state structures of **9** (left), and **10** (right) [green = fluorine). Selected bond lengths [Å] and angles [°]: **9**, Sb1 C1 2.207(2), Sb1 C14 2.202(2), Sb1 C27 2.181(2), C14 Sb1 C1 101.89(9), C27 Sb1 C1 100.21(9), C27 Sb1 C14 92.43(8); **10**, Sb1 C14 2.1702(19), Sb1 C1 2.208(2), Sb1 C20 2.175(2), C14 Sb1 C1 99.9(1), C14 Sb1 C20 92.2(1), C20 Sb1 C1 103.5(1).

Given the success with $Sb(C_6F_5)_3$ as the substrate, we were wondering whether $PhSb(C_6F_5)_2$ (**11**) and $Ph_2SbC_6F_5$ (**12**) both being significantly less electron-deficient than $Sb(C_6F_5)_3$ [8a] would engage in base-catalyzed reactions with weakly acidic hydrocarbons as well. Gratifyingly, **11** smoothly reacted with two equivalents of phenyl acetylene in the presence of 5 mol% of **P_1-But** to furnish disubstituted stibine **13** in almost quantitative yields (Figure 3). The reaction proceeds with high selectivity, only the C_6F_5 moieties are replaced by the phenyl acetylide group through base catalysis while the phenyl group bound to the antimony center is not affected. Furthermore, **13** proved to be an excellent precursor for the formation of the first isolated 1,4-stibaborine derivatives **14** and **15** [26, 27]. Both were synthesized in 28% and 53% yield by treatment of **13** with $B(C_6F_5)_3$ and BPh_3, respectively, via a two-fold Wrackmeyer reaction (1,1-carbaboration) [28]. The results of a single crystal X-ray analysis of **14** confirmed the presence of a six-membered ring with antimony and boron in the 1,4 position (Figure 3). The stibaborine ring exhibits a boat conformation with the C=C, Sb-C, and B-C bond lengths being in the expected range.

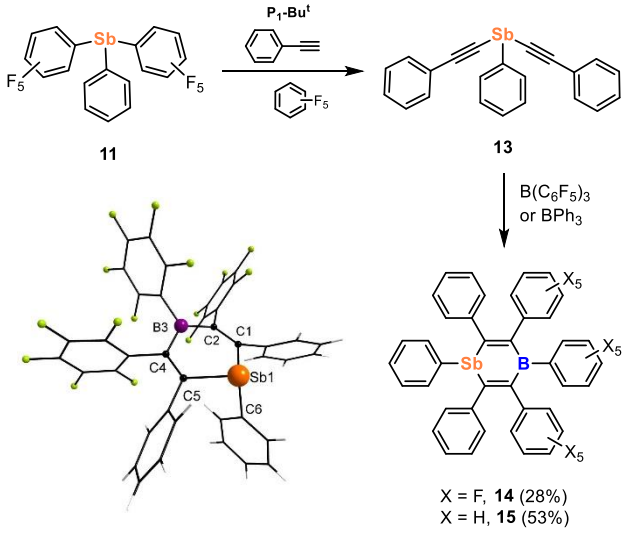

Figure 3. Formation of **13** and its conversion to the stibaborines **14** and **15.** Solid-state structure of **14**. Selected bond lengths [Å] and angles [°]: Sb1 C1 2.145(2), Sb1 C5 2.155(2), Sb1 C6 2.155(3), C1 C2 1.352(3), C2 B3 1.557(4), B3 C4 1.555(4), C4 C5 1.350(4), C1 Sb1 C5 94.5(1), C1 Sb1 C6 92.7(1), C6 Sb1 C5 94.1(1), C4 B3 C2 123.9(2).

Alkynyl-substituted stibines have recently emerged as reagents with potential in synthetic organic chemistry spanning from copper-catalyzed Huisgen [29, 30] to metal-catalyzed cross-coupling reactions [10]. With this in mind, we were pleased to see that $Ph_2SbC_6F_5$ (**12**) readily reacted at room temperature with phenyl acetylene under base catalysis to generate stibine **16** nearly quantitatively in solution as confirmed by ^{1}H and ^{19}F NMR spectroscopy (Scheme 5).

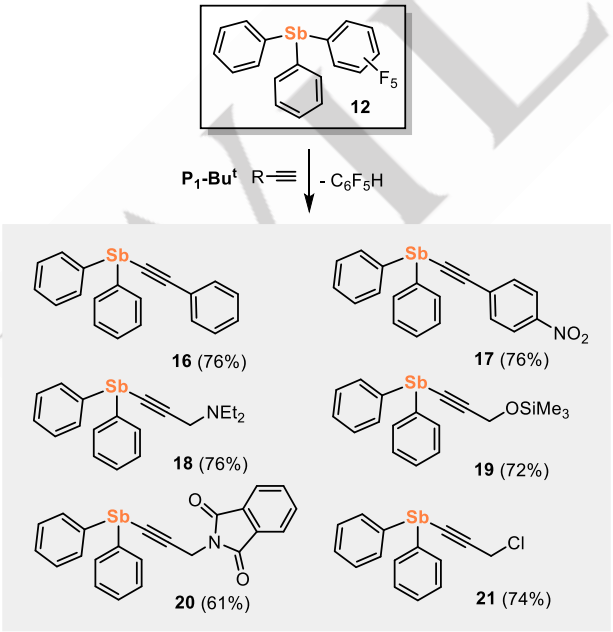

Scheme 5. Base-catalyzed formation of **16**-**21**.

Next, we tested our method on various alkyne substrates decorated with organic functional groups and noticed that ester, nitro, chloro, amide, amino, and siloxy groups were well tolerated by the catalyst system at room temperature in toluene to give the respective stibines **17**-**21** in good isolated yields. Acetylene could be utilized as a substrate for Sb-C bond formation as well; in this case, bis stibine **22** was isolated as the major product in ca. 50% yield (Figure 6) [31]. Single crystal X-ray diffraction analysis of crystals **22** grown from C_6D_6 (Figure 4) unequivocally confirmed the assumed structure. As expected, the Sb1-$C1_{(alkyne)}$ bonds [1.211(12) Å] were found to be somewhat shorter than the Sb1-$C2_{(aryl)}$ [2.157(7)Å] and Sb1-$C8_{(aryl)}$ [2.159(8) Å] distances.

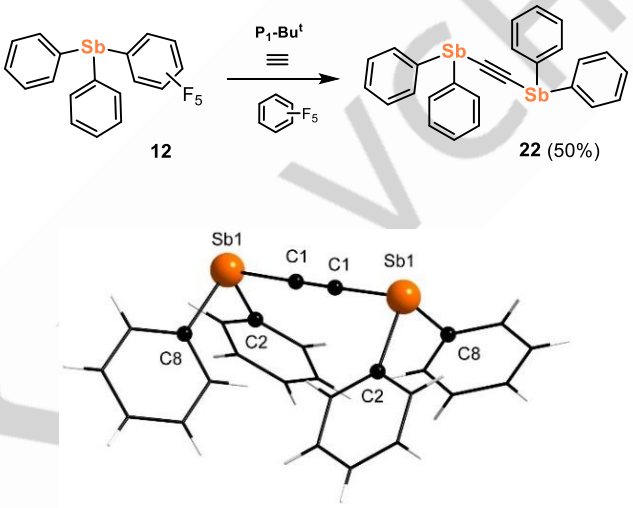

Figure 4. Base-catalyzed formation and solid-state structure of **22**. Selected bond lengths [Å] and angles [°]: Sb1 C1 2.108(6), Sb1 C2 2.157(7), Sb1 C8 2.159(8), C1 C1 1.211(12), C1 Sb1 C2 94.4(4), C1 Sb1 C8 93.2(3), C2 Sb1 C8 94.1(3), C1 C1 Sb1 179.2(5).

To further demonstrate the potential of pentafluorophenyl-substituted stibines as chemical reagents, we performed a two-step sequential reaction of **12** with HC≡CCOOEt under base catalysis followed by a 1,1-carbaboration via subsequent addition of $B(C_6F_5)_3$ (Scheme 6). The corresponding product, stibine **24**, was isolated as a crystalline material with an overall yield of 48% and was fully characterized by multi-nuclear NMR spectroscopy. The ^{11}B NMR spectrum of **24** exhibits a signal at -5.0 ppm indicating tetra-coordination of the boron atom, while the ^{19}F NMR shows two sets of three fluorine signals in a 2:1 ratio confirming migration of one of the C_6F_5 groups from boron to carbon. Single-crystal X-ray diffraction analysis of **24** confirmed the assumed connectivity with the migrated C_6F_5 group and the $B(C_6F_5)_2$ moiety both being bound at the β-carbon (C1) of the alkynoate (Figure 5). Consistent with the ^{11}B NMR spectroscopic results, the carbonyl oxygen coordinates to the boron atom [B1-O1, 1.554(3) Å] resulting in a tetrahedral coordination environment for the central boron. Notably, the formation of **24** represents the first example of an ethynyl-substituted stibine engaging in a 1,1-carboration reaction. In contrast, silyl analog, $Me_3SiC{\equiv}CCOOEt$, forms a Lewis acid-base adduct with $B(C_6F_5)_3$ [32] and aryl/alkyl-

substituted alkynoates undergo a 1,2-*anti*-carboration with aliphatic organoboranes [33].

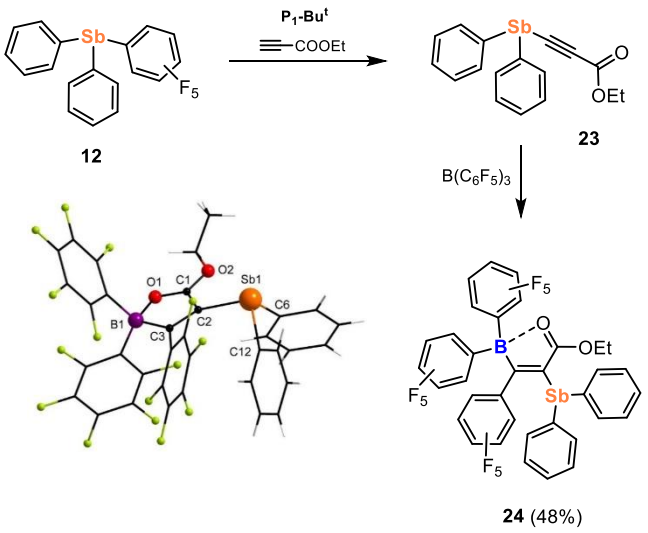

Figure 5. Formation and solid-state structure of **24** (green = fluorine). Selected bond lengths [Å] and angles [°]: Sb1 C2 2.160(2), Sb1 C6 2.149(2), Sb1 C12 2.150(2), O1 C1 1.273(3), O1 B1 1.554(3), O2 C1 1.289(3), C1 C2 1.454(3), C3 C2 1.362(3), C3 B1 1.647(3), C6 Sb1 C2 98.0(1), C6 Sb1 C12 90.3(1), C12 Sb1 C2 98.1(1).

To gain mechanistic insights into the base-catalyzed antimony-carbon bond-formation event, kinetic measurements of a model reaction were performed using ^{19}F NMR spectroscopy (eq. 1). The results imply the empirical rate law to exhibit an approximately first-order dependence on **P$_1$-Bu^t** (cat.), PhC≡CH, and $Ph_2SbC_6F_5$ (eq. 2, Figure 6a−c). For the full kinetic equation treatment, please see the Supporting Information. Deuterium isotope studies show that the reaction exhibits a KIE (k_H/k_D) of 1.2 (Figure 6d) suggesting the C-H bond activation of the alkyne to be involved in the operative turnover-limiting step. These findings appear to be in line with the observation that the rate of the reaction is accelerated with increasing basicity of the base.

$$Ph_2SbC_6F_5 + PhC{\equiv}CH \rightarrow Ph_2SbC{\equiv}CPh + C_6F_5H \qquad \text{(eq. 1)}$$

$$\delta p/\delta t = k_{obs} \times [\mathbf{P_1\text{-}Bu^t}]^1[PhC{\equiv}CH]^{1.3}[Ph_2SbC_6F_5]^1 \qquad \text{(eq. 2)}$$

To further elucidate the reaction mechanism of this novel organic superbase-catalyzed Sb-C bond formation reaction and its selectivity, density functional theory calculations (DFT) on the model reaction shown in equation 1 were carried out using a B3LYP-D hybrid functional with def2-SVP basis set [34] utilizing the program package ORCA [35]. The transition state was located through the nudged elastic band (NEB) method, where the path between the reactants and products was discretized into a series of structural images [36]. The image closest to the transition state was completely optimized in a transition state search and its character was confirmed by one imaginary frequency.

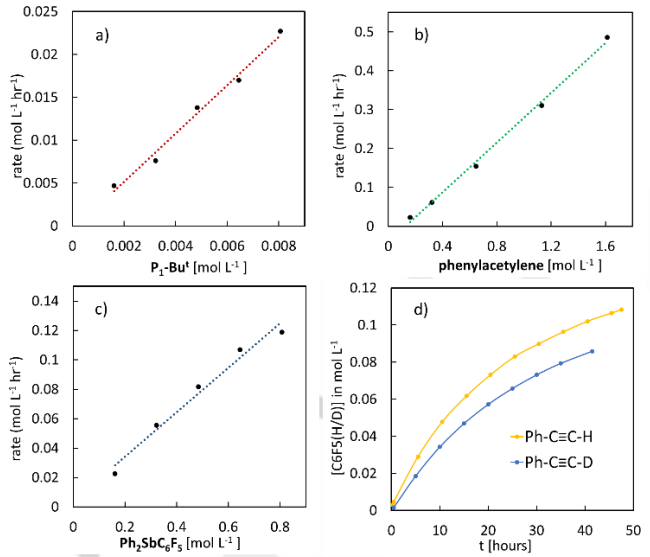

Figure 6. The plot of initial reaction rate δp/δt against the concentration of (a) **P$_1$-Bu^t**, (b) phenyl acetylene, and (c) $Ph_2SbC_6F_5$ for the **P$_1$-Bu^t**-catalyzed reaction of $Ph_2SbC_6F_5$ with PhC≡CH (d) Plot of concentration of C_6F_5H/D vs time for the **P$_1$-Bu^t**-catalyzed reaction of $Ph_2SbC_6F_5$ with PhC≡CH and PhC≡CD, respectively.

The computed free-energy profile along with the calculated Van der Waals complexes of the reactants and products as well as the transition state structure are shown in Figure 7. The catalytic process is slightly exergonic (-3.2 kcal/mol) and proposed to proceed most likely via a concerted σ-bond metathesis mechanism [37]. The proposed transition state features a 4-membered ring structure involving antimony, the ipso-carbon of the C_6F_5 substituent as well as hydrogen and carbon of the alkyne substrate. In the transition state, the base catalyst, **P$_1$-Bu^t**, activates the Sb-C bond of $Ph_2SbC_6F_5$ but not the C-H bond of the alkyne. Note also that the catalysts imine nitrogen (N=P) strongly interacts with the antimony center most likely through pnictogen bonding resulting in a short Sb-N distance of 231 pm. In addition, one of the catalysts pyrrolidino groups is in proximity to the central antimony as well with a Sb-N distance of 307 pm. These secondary bond interactions appear to be responsible for a substantial weakening of the Sb-C_6F_5 bond (Sb-C_{ipso}, 293 pm), facilitating the transfer of the proton directly from phenyl acetylene to the C_6F_5 group with simultaneous liberation of the products C_6F_5H and $Ph_2SbC{\equiv}CPh$.

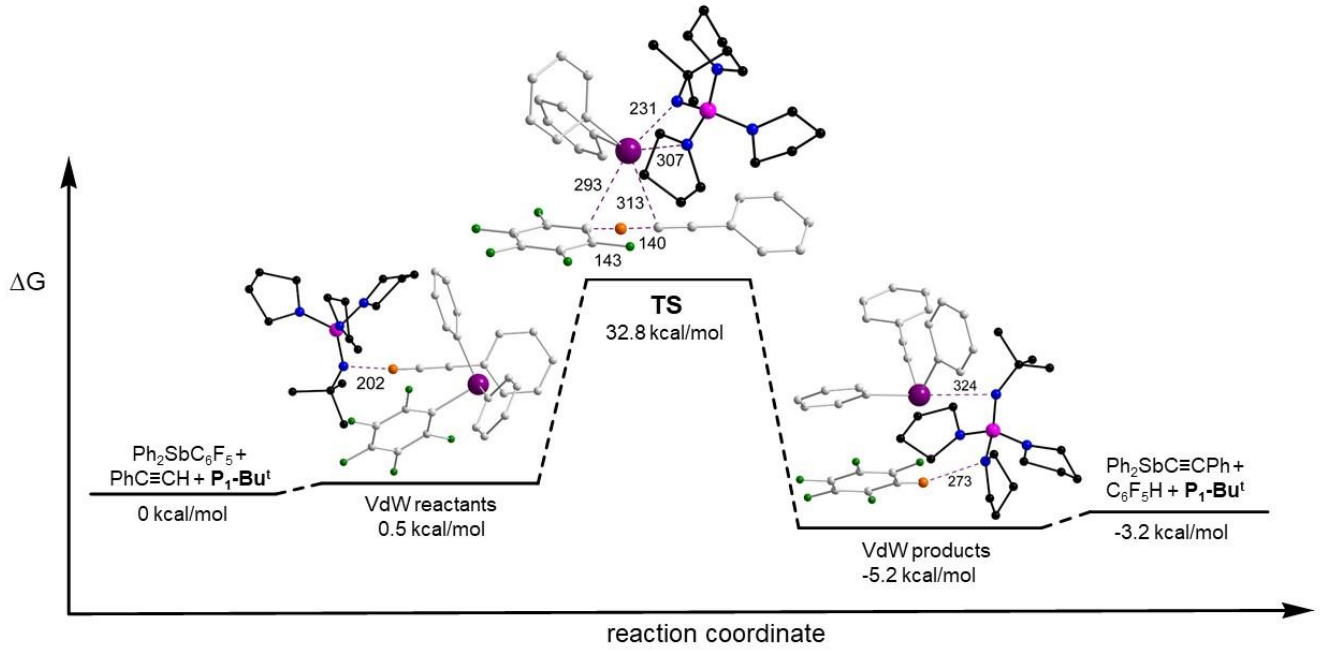

Figure 7. Computed free energy profile (kcal/mol) and optimized structure of the transition state (TS) for the organic superbase-catalyzed Sb-C bond formation. Selected bond lengths of the transition state structure and the Van der Waals complexes of the products and reactants are shown in pm and non-pertinent hydrogen atoms are omitted for clarity (colour coding of the atoms: purple = antimony, pink = phosphorus, blue = nitrogen, green = fluorine, orange = hydrogen, black = carbons of the base catalyst, grey = carbons of the substrates and products).

Conclusion

For the first time, the ability to selectively construct antimony-carbon bonds via organic superbase catalysis under metal- and salt-free conditions was demonstrated. This novel catalytic approach provides facile access to a range of new aromatic and heteroaromatic organostibines under mild conditions. In addition, various mono-, di- and tri-substituted organostibines decorated with organic functional groups at the alkyne moiety could easily be synthesized, which are difficult to access via standard organometallic synthetic approaches. Notably, the C_6F_5-group serves as the leaving group in this catalytic transformation, which is liberated from the stibine substrate upon formal protonation as C_6F_5H, a volatile liquid that can easily be separated from the product. This allows the progress of the Sb-C bond formation to be easily monitored by ^{19}F-NMR spectroscopic methods. Computations support the experimental reaction conditions with a pathway proposed to proceed via a concerted σ-bond metathesis transition state, where the base catalyst appears to activate the Sb-C_6F_5 bond sequence through secondary bond interactions (pnictogen bonding).

Collectively, we think that this highly selective and catalytic metal- and salt-free Sb-C bond formation approach introduced herein will open new opportunities to further explore the chemistry, properties and applications of organoantimony compounds; work in this chemical space is currently ongoing.

Supporting Information

The supporting information contains detailed experimental procedures, X-ray crystallography data, DFT calculations results and NMR spectroscopic data. Deposition numbers CCDC-2284712 (for **22**); CCDC-2284713 (for **9**); CCDC-2284714 (for **10**); CCDC-2284715 (for **4**); CCDC-2284716 (for **3**); CCDC-2284717 (for **24**); CCDC-2284718 (for **14**) and CCDC-2284735 (for **8**) contain the supplementary crystallographic data for this paper. These data are provided free of charge by the joint Cambridge Crystallographic Data Centre and Fachinformations-zentrum Karlsruhe Access Structures service.

Acknowledgements

This research was supported by the U.S. Department of Energy, Office of Science, Office of Basic Energy Sciences, Catalysis Science Program, under Award DE-SC0019094.

Conflict of Interest

The authors declare no conflict of interest.

Data Availability Statement

The data that support the findings of this study are available in the supplementary material of this article.

Keywords: Antimony • Pnictogen Bonding • Superbase Catalysis • Metal Free Catalysis • Organocatalysis

[1] a) M. Hirai, F.P. Gabbai, *Angew. Chem., Int. Ed.* **2015**, *54*, 1205-1209; b) A.M. Christianson, F. P. Gabbai, *Organometallics* **2017**, *36*, 3013-3015; c) A.M. Christianson, E. Rivard, F.P. Gabbai, *Organometallics* **2017**, *36*, 2670-2676; d) C.-H. Chen, F.P. Gabbai, *Angew. Chem., Int. Ed*. **2017**, *56*, 1799-1804; e) H. Kuhn, A. Docker, P.D. Beer, *Chem. Eur. J.* **2022**, *28*, e20220183; f) J.L. Beckmann, J. Krieft, Y.V. Vishnevskiy, B. Neumann, H.-G. Stammler, N.W. Mitzel, *Chem. Sci.* **2023**, *14*, 13551-13559; g) Beckmann, J.L.; Krieft, J.; Vishnevskiy, Y.V.; Neumann, B.; Stammler, H.-G.; Mitzel, N. W. *Angew. Chem., Int. Ed.* **2023**, *62*, e202310439.

[2] a) L.-S. Ke, M. Myahkostupov, F.N. Castellano, F.P. Gabbai, *J. Am. Chem. Soc.* **2012**, *134*, 15309-15311; b) M. Hirai, F.P. Gabbai, *Chem. Sci.* **2014**, *5*, 1886-1893; c) M. Hirai, M. Myahkostupov, F.N. Castellano, F.P. Gabbai, *Organometallics* **2016**, *35*, 1854-1860; d) A.M. Christianson, F.P. Gabbai, *Chem. Commun.* **2017**, *53*, 2471-2474; e) A. Kumar, M. Yang, M. Kim, F.P. Gabbai, M. H. Lee, *Organometallics* **2017**, *36*, 4901-4907; f) L. Li, Y. Zhang, Y. Li, Y. Duan, Y. Qian, P. Zhang, Q. Guo, J. Ding, *ACS Sensors* **2020**, *5*, 3465-3473.

[3] a) L.M. Lee, M. Tsemperouli, A.I. Poblador-Bahamonde, S. Benz, N. Sakai, K. Sugihara, S. Matile, *J. Am. Chem. Soc.* **2019**, *141*, 810-814; b) G. Park, D.J. Brock, J.-P. Pellois, F.P. Gabbai, Chem **2019**, *5*, 2215-2227; c) G. Park, F.P. Gabbai, *Chem. Sci.* **2020**, *11*, 10107-10112.

[4] a) J. Ohshita, R. Fujita, D. Tanaka, Y. Ooyama, N. Kobayashi, *Chem. Lett.* **2012**, *41*, 1002–1003; b) J. Ohshita, K. Yamaji, Y. Ooyama, Y. Adachi, M. Nakamura, S. Watase, *Organometallics* **2019**, *38*, 1516–1523; c) M. Matsumura, Y. Matsuhashi, M. Kawakubo, T. Hyodo, Y. Murata, M. Kawahata, K. Yamaguchi, S. Yasuike, *Molecules* **2021**, *26*, 222; d) R. Inaba, K. Oka, T. Iwami, Y. Miyake, K. Tajima, H. Imoto, K. Naka, *Inorg. Chem.* **2022**, *61*, 7318–7326; e) G.R. Kumar, M. Yang, B. Zhou, F.P. Gabbaï, *Mendeleev Commun*. **2022**, *32*, 66-67; f) T. Fujii, A. Urushizaki, H. Imoto, K. Naka, *Asian J. Chem.* **2023**, *12*, e202300067.

[5] a) H. Yang, FP. Gabbai, *J. Am. Chem. Soc.* **2015**, *137*, 13425-13432; b) D. You, F. P. Gabbai, *J. Am. Chem. Soc.* **2017**, *139*, 6843-6846; c) D. You, H. Yang, S. Sen, F.P. Gabbai, *J. Am. Chem. Soc.* **2018**, *140*, 9644-9651; d) Y.-H. Lo, F.P. Gabbai, *Angew. Chem., Int. Ed.* **2019**, *58*, 10194-10197.

[6] a) H. Yang, F.P. Gabbai, *J. Am. Chem. Soc.* **2014**, *136*, 10866-10869; b) B. Pan, F.P. Gabbai, *J. Am. Chem. Soc.* **2014**, *136*, 9564-9567; c) B. Zhou, F.P. Gabbai, *J. Am. Chem. Soc.* **2023**, *145*, 13758-13767.

[7] For catalysis with organoantimony(V) compounds: a) J. Xia, R. Qiu, S. Yin, X. Zhang, S. Luo, C.-T. Au, K. Xia, W.-Y. Wong, *J. Organomet. Chem.* **2010**, *695*, 1487–1492; b) M. Hirai, J. Cho, F.P. Gabbaï, *Chem. Eur. J.* **2016**, *22*, 6537–6541; c) R. Arias Ugarte, T.W. Hudnall, *Green Chem.* **2017**, *19*, 1990-1998; d) N. Tan, T. Nie, C.-T. Au, D. Lan, S. Wu, B. Yi, *Tetrahedron Lett.* **2017**, *58*, 2592-2595; e) M. Yang, M. Hirai, F.P. Gabbaï, *Dalton Trans.* **2019**, *48*, 6685–6689; f) J. Lei, L. Peng, R. Qiu, Y. Liu, Y. Chen, C.-T. Au and S.-F. Yin, *Dalton Trans.* **2019**, *48*, 8478-8487; g) J. Zhang, J. Wei, W.-Y. Ding, S. Li, S. H. Xiang, B. Tan, *J. Am. Chem. Soc.* **2021**, *143*, 6382–6387.

[8] For catalysis with organoantimony(III) compounds: a) S. Benz, A. I. Poblador-Bahamonde, N. Low-Ders, S. Matile, *Angew. Chem., Int. Ed.* **2018**, *57*, 5408-5412; b) A. Gini, M. Paraja, B. Galmes, C. Besnard, A.I. Poblador-Bahamonde, N. Sakai, A. Frontera, S. Matile, *Chem. Sci.* **2020**, *11*, 7086-7091; c) M. Paraja, A. Gini, N. Sakai, S. Matile, *Chem. Eur. J.* **2020**, *26*, 15471-15476; d) H.V. Humeniuk, A. Gini, X. Hao, F. Coelho, N. Sakai, S. Matile, *J. Am. Chem. Soc. Au* **2021**, *1*, 1588-1593; e) D. Sharma, A. Benny, R. Gupta, E.D. Jemmis, A. Venugopal. *Chem. Commun.* **2022**, *58*, 11009-11012.

[9] a) N. Kakusawa, K. Yamaguchi, J. Kurita, T. Tsuchiya, *Tetrahedron Lett.* **2000**, *41*, 4143-4146; b) N. Kakusawa, Y. Tobiyasu, S. Yasuike, K. Yamaguchi, H. Seki, J. Kurita, *Tetrahedron Lett.* **2003**, *44*, 8589-8592; c) N. Kakusawa, K. Yamaguchi, J. Kurita, *J. Organomet. Chem.* **2005**, *690*, 2956–2966; d) N. Kakusawa, Y. Tobiyasu, S. Yasuike, K. Yamaguchi, H. Seki, J. Kurita, *J. Organomet. Chem.* **2006**, *691*, 2953–2968; b) N. Kakusawa, J. Kurita, *Chem. Pharm. Bull.* **2006**, *54*, 699-702; e) Q. Simpson, M. J. G. Sinclair, D. W. Lupton, A. B. Chaplin, J. F. Hooper, *Org. Lett.* **2018**, *20*, 5537−5540; f) Y. Murata, N. Kakusawa, Y. Arakawa, Y. Hayashi, S. Morinaga, M. Ueda, T. Hyodo, M. Matsumura, K. Yamaguchi, J. Kurita, S. Yasuike, *J. Organomet. Chem.* **2020**, *928*, 121545; g) Z. Zhang, D. Zhang, L. Zhu, D. Zeng, N. Kambe, R. Qiu, *Org. Lett.* **2021**, *23*, 5317-5322.

[10] a) L. Le, S. Li, D. Zhang, S.-F. Yin, N. Kambe, R. Qiu, *Org. Lett.* **2022**, *24*, 6159-6164; b) D. Zhang, Z. Xu, T. Tang, L. Le, C. Wang, N. Kambe, R. Qiu, *Org. Lett.* **2022**, *24*, 3155-3160; c) D. Zhang, T. Tang, Z. Zhang, L. Le, Z. Xu, H. Lu, Z. Tong, D. Zeng, W.-Y. Wong, S.-F. Yin, A. Ghaderi, N. Kambe, R. Qiu, *ACS Catal.* **2022**, *12*, 854-867.

[11] a) K.-Y. Akiba and Y. Yamamoto, The Chemistry of Organic Arsenic, Antimony and Bismuth Compounds, Wiley, New York, **1994**; b) H. J. Breunig and R. Rösler. *Coord. Chem. Rev.* **1997**, *163*, 33-53; c) Comprehensive Organometallic Chemistry IV (Fourth Edition) Vol 10, **2022**, 478-522, 10.05 - Organometallic Compounds of Arsenic, Antimony and Bismuth, J. Cornella, Y. Pang.

[12] a) M. Bonaterra, S.E. Martin, R.A. Rossi, *Org. Lett.* **2003**, *5*, 2731-2734; b) M. Bonaterra, R.A. Rossi, S.E. Martín, *Organometallics* **2009**, 28, 933-936.

[13] a) D. Zhang, L. Le, R. Qiu, W.-Y. Wong, N. Kambe, Angew. *Chem., Int. Ed.* **2021**, *60*, 3104–3114; b) d) L. Le, M. Yin, H. Zeng, W. Xie, W. Zhou, Y. Chen, B. Xiong, S.-F. Yin, N. Kambe, R. Qiu, *Org. Lett.* **2024**, *26*, 344-349.

[14] T. Tang, D. Zhang, L. Le, Z. Xu, H. Lu, S.-F. Yin, N. Kambe, R. Qiu, *J. Organomet. Chem.* **2022**, *973-974*, 122352.

[15] a) G.C. Welch, R.R.S. Juan, J.D. Masuda, D.W. Stephan, *Science* **2006**, *314*, 1124-1126; b) G.C. Welch, D.W. Stephan, *J. Am. Chem. Soc.* **2007**, *129*, 1880-1881; c) P. Spies, G. Erker, G. Kehr, K. Bergander, R. Fröhlich, S. Grimme, D.W. Stephan, *Chem. Commun.* **2007**, 5072–5074.

[16] M. Yang, D. Tofan, C.-H. Chen, K.M. Jack, F.P. Gabbai, *Angew. Chem., Int. Ed.* **2018**, *57*, 13868-13872.

[17] a) R. Schwesinger, *Chimia* **1985**, *39*, 269-72; b) R. Schwesinger, J. Willaredt, H. Schlemper, M. Keller, D. Schmitt, H. Fritz, *Chem. Ber.* **1994**, *127*, 2435-54; c) J.G. Verkade, P.B. Kisanga, *Aldrichim. Acta* **2004**, *37*, 3-14; d) Superbases for Organic Synthesis: Guanidines, Amidines, Phosphazenes and Realted Organocatalysts, Ishikawa, T., Ed.; Wiley, Chichester, UK, **2009**; d) K. Vazdar, D. Margetic, B. Kovacevic, J. Sundermeyer, I. Leito, U. Jahn, *Acc. Chem. Res.* **2021**, *54*, 3108; e) T.R. Puleo, S.J. Sujansky, S.E. Wright, J.S. Bandar, *Chem. Eur. J.* **2021**, *27*, 4216.

[18] Selected examples of superbase catalysis: a) T. Imahori, Y. Kondo, *J. Am. Chem. Soc.* **2003**, *125*, 8082–8083; b) E. Blondiaux, J. Pouessel, T. Cantat, *Angew. Chem., Int. Ed.* **2014**, *53*, 12186-12190; c) C. Luo, J.S. Bandar, *J. Am. Chem. Soc.* **2018**, *140*, 3547-3550; d) M. Shigeno, K. Hayashi, K. Nozawa-Kumada, Y. Kondo, *Org. Lett.* **2019**, *21*, 5505–5508; e) Y.-H. Wang, Z.-Y. Cao, Q.-H. Li, G.Q. Lin, J. Zhou, P. Tian, *Angew. Chem., Int. Ed.* **2020**, *59*, 8004; f) S. H. Doan, N. N. H. Ton, B. K. Mai, T. V. Nguyen, *ACS Catal.* **2022**, *12*, 12409-12418; g) C. Luo, J.V. Alegre-Requena, S.J. Sujansky, S.P. Pajk, L.C. Gallegos, R.S. Paton, J.S. Bandar, *J. Am. Chem. Soc.* **2022**, *144*, 9586-9596.

[19] a) S. Mummadi, A. Brar, G. Wang, D. Kenefake, R. Diaz, D.K. Unruh, S. Li, C. Krempner, C. *Chem. Eur. J.* **2018**, *24*, 16526–16531; b) S. Mummadi, D.K. Unruh, J. Zhao, S. Li, C. Krempner, *J. Am. Chem. Soc.* **2016**, *138*, 3286–3289; c) S. Mummadi, C. Krempner, *Molecules* **2023**, *28*, 1340-57; d) S. Mummadi, D. Kenefake, R. Diaz, D.K. Unruh, C. Krempner, *Inorg. Chem.* **2017**, *56*, 10748-10759; e) H. Li, A.J. Aquino, D.B. Cordes, F. Hung-Low, W.L. Hase, C. Krempner, *J. Am. Chem. Soc.* **2013**, *135*, 16066-16069.

[20] W.S. Matthews, J.E. Bares, J.E. Bartmess, F.G. Bordwell, F.J. Cornforth, G.E. Drucker, Z. Margolin, R.J. McCallum, G.J. McCollum, N. R. Vanier, *J. Am. Chem. Soc.* **1975**, *97*, 7006-7014.

[21] a) H. Hartmann, W. Reiss, B. Karbstein, Naturwiss. **1959**, *46*, 321; b) D. Mootz, P. Holst, L. Berg, K.Z. Drews, *Kristallogr. – Cryst. Mater.* **1962**, *117*, 233-234.

[22] No reaction was observed when only $Sb(C_6F_5)_3$ and phenyl acetylene were reacted in C_6D_6 as solvent even at 80°C.

[23] K. Shen, Y. Fu, J.-N. Li, L. Liu, Q.-X. Guo, *Tetrahedron* **2007**, *63*, 1568-1576.

[24] a) H.A. Bent, *Chem. Rev.* **1968**, *68*, 587–648; b) N.W. Alcock, *Adv. Inorg. Chem. and Radiochem.* **1972**, *15*, 1–58.

[25] a) M. Mantina, A.C. Chamberlin, R. Valero, C.J. Cramer, D.G. Truhlar, *J. Phys. Chem. A*, **2009**, *113*, 5806-5812; b) P. Pyykkö, M. Atsumi, *Chem. Eur. J.* **2009**, *15*, 186-197.

[26] P.A. Brown, C.D. Martin, K.L. Shuford, *Phys. Chem. Chem. Phys.* **2019**, *21*, 18458-18466.

[27] a) F.A. Tsao, A.J. Lough, D.W. Stephan, *Chem. Commun.* **2015**, 51, 4287-4289; b) F.A. Tsao, D.W. Stephan, *Dalton Trans.* **2015**, 44, 71-74.

[28] a) B. Wrackmeyer, Coord. *Chem. Rev.* **1995**, *145*, 125-156; b) B. Wrackmeyer, *Het. Chem.* **2006**, *17*, 188-208; c) G. Kehr, G. Erker, *Chem. Commun.* **2012**, *48*, 1839-1850.

[29] a) R. Huisgen, *Proc. Chem. Soc.*, **1961**, 357-396; b) H.C. Kolb, M.G. Finn, K.B. Sharpless, *Angew. Chem. Int. Ed.* **2001**, *40*, 2004–2021.

[30] a) M. Yamada, T. Takahashi, M. Hasegawa, M. Matsumura, K. Ono, R. Fujimoto, Y. Kitamura, Y. Murata, N. Kakusawa, M. Tanaka, T. Obata, Y. Fujiwara, S. Yasuike, *Bioorg. & Med. Chem. Lett.* **2018**, *28*, 152-154; b) M. Yamada, D. Matsuura, M. Hasegawa, Y. Murata, N. Kakusawa, M. Matsumura, S. Yasuike, *J. Organomet. Chem.* **2018**, *871*, 79-85; c) M. Yamada, M. Matsumura, F. Takino, Y. Murata, Y. Kurata, M. Kawahata, K. Yamaguchi, N. Kakusawa, S. Yasuike, *Eur. J. Org. Chem.* **2018**, *2018*, 170-177; d) M. Yamada, M. Matsumura, Y. Uchida, M. Kawahata, Y. Murata, N. Kakusawa, K. Yamaguchi, S. Yasuike, Beilstein *J. Org. Chem.* **2016**, *12*, 1309-1313.

[31] H. Hartmann, C. Beermann, Germany, DE1062244, **1959**-07-30.

[32] J.Z. Chan, A. Yesilcimen, M. Cao, Y. Zhang, B. Zhang, M. Wasa, *J. Am. Chem. Soc.* **2020**, *142*, 16493-16505.

[33] a) K. Nagao, H. Ohmiya, M. Sawamura, *J. Am. Chem. Soc.* **2014**, *136*, 10605-10608; b) A. Yamazaki, K. Nagao, T. Iwai, H. Ohmiya, M. Sawamura, *Angew. Chem., Int. Ed.* **2018**, *57*, 3196-3199.

[34] F. Weigend, R. Ahlrichs, *Phys. Chem. Chem. Phys.* **2005**, *7*, 3297-3305.

[35] a) F. Neese, WIREs Computational Molecular Science **2012**, *2*, 73-78; b) F. Neese, F. Wennmohs, U. Becker; C. Riplinger, *J. Chem. Phys.* **2020**, *152*, 224108.

[36] V. Ásgeirsson, B. O. Birgisson, R. Bjornsson, U. Becker, F. Neese, C. Riplinger, H. Jónsson, *J. Chem. Theory Comput.* **2021**, 17, 8, 4929-4945.

[37] R. Watermann, Organometallics **2013**, *32*, 7249-7263.

Entry for the Table of Contents

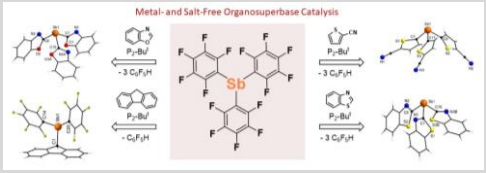

C_6F_5, the perfect leaving group for highly selective antimony-carbon bond formation reactions via organosuperbase-catalysis! This novel approach enables mono-, di- and tri-substituted perfluorophenyl stibines to be smoothly converted to a range of synthetically useful aromatic, heteroaromatic and alkynyl-substituted stibines under metal- and salt-free conditions.